

October 1970

LRP 42/70

CENTRE DE RECHERCHES EN PHYSIQUE DES PLASMAS  
FINANCÉ PAR LE FONDS NATIONAL SUISSE DE LA RECHERCHE SCIENTIFIQUE

STUDY OF SHORT WAVELENGTH INSTABILITIES IN THE CONFINEMENT  
OF A COLLISION DOMINATED PLASMA BY A ROTATING MAGNETIC FIELD

F. Troyon

LAUSANNE

October 1970

LRP 42/70

CENTRE DE RECHERCHES EN PHYSIQUE DES PLASMAS  
FINANCÉ PAR LE FONDS NATIONAL SUISSE DE LA RECHERCHE SCIENTIFIQUE

STUDY OF SHORT WAVELENGTH INSTABILITIES IN THE CONFINEMENT  
OF A COLLISION DOMINATED PLASMA BY A ROTATING MAGNETIC FIELD

F. Troyon

LAUSANNE

October 1970

LRP 42/70

STUDY OF SHORT WAVELENGTH INSTABILITIES IN THE CONFINEMENT  
OF A COLLISION DOMINATED PLASMA BY A ROTATING MAGNETIC FIELD

F. Troyon

A b s t r a c t

A collision dominated plasma confined by a rotating magnetic field is stable if  $f > .02 \nu_1$  where  $f$  is the frequency of rotation and  $\nu_1$  the ion collision frequency. Short wavelength perturbations are the most difficult to stabilize. Growth rates of parametric instabilities are shown to be so large as to make impossible any attempt to use a frequency much lower than the above limit. A simple interpretation of a wide region of instability, which cannot be ascribed to any parametric instability, is given in terms of an equivalent negative resistance.

Lausanne

## Introduction

A rotating magnetic field pinch consists of a superposition of oscillating  $\theta$  and  $z$  pinches,  $90^\circ$  out of phase and of intensities such that the field amplitude on the plasma surface remains constant in time. Such a configuration is presently being studied experimentally<sup>1-2</sup> and theoretically<sup>3-5</sup>. In a previous paper (ref. 4) it is shown that, for a collision dominated plasma, the frequency necessary to obtain stability of all modes of deformation of the plasma surface is of the order of the ion-ion collision frequency. Such a high frequency is required to stabilize the short wavelengths, the long wavelengths being stable at a much lower frequency.

The aim of this work is to calculate numerically the stability diagram for the short wavelengths in order to determine precisely the minimum frequency needed to obtain stability and to find if the maximum growth rates in the unstable regime are acceptable. It also presents a simple physical interpretation of the various instabilities which are uncovered. In particular it is shown that the stability analysis at high frequency can be carried through using a more general method than the usual time averaging procedure<sup>7</sup> which can only be used for simple systems (Mathieu-Hill equations for example).

## The Model

Consider a sharp boundary plasma which fills a half space  $z > 0$ , with no field inside the plasma. A rotating magnetic field  $\underline{B}$  fills the other half space  $z < 0$ :

$$B_x = B \cos \omega t, \quad B_y = B \sin \omega t$$

To describe the plasma behaviour we use the Navier-Stokes equations for a viscous gas obeying an adiabatic law  $p\rho^{-\gamma} = \text{constant}$ . The thermal conductivity is assumed to be zero; however the case of infinite thermal conductivity can be simulated by taking  $\gamma = 1$ . We estimate the influence of finite conductivity by comparing the results for the two cases  $\gamma = 5/3$  and  $\gamma = 1$ . Denote by  $\mu$  the viscosity (the second coefficient of viscosity is assumed to be zero),  $p_0$  the pressure,  $\rho_0$  the density and  $u = \sqrt{\gamma p_0 / \rho_0}$  the sound velocity of the plasma.  $\alpha = \mu / (\rho_0 u)$  has the dimension of a length to which corresponds the characteristic frequency  $\nu = u / \alpha$ .

For a perturbation of the plasma surface of the form

$$z = \varepsilon(t) e^{iHx}$$

we obtain the equation of motion (ref. 4)

$$X (1 + \cos 2\omega t) \varepsilon(t) + \int_0^t R(t-t') \dot{\varepsilon}(t') dt' = 0 \quad (1)$$

where  $X = uHp_0$ , and  $R(t)$  is defined through its Laplace transform:

$$\begin{aligned} \tilde{R}(s) &= \int_0^{\infty} dt e^{-st} R(t) \\ \tilde{R}(s) &= \frac{\rho_0 s}{k_L} + 4\alpha^2 \gamma p_0 H^2 \frac{k_T^2 - k_T k_L}{s k_L} \end{aligned} \quad (2)$$

$$k_L^2 = H^2 + \frac{s^2 / u^2}{1 + \frac{4}{3} \alpha s / u} \quad ; \quad k_T^2 = H^2 + \frac{s}{\alpha u}$$

Stability

We introduce the normalized variables

$$\beta = \alpha H, \quad \Omega = \frac{2\omega}{v}, \quad \underline{s} = s/v, \quad \underline{k}_L = \alpha k_L, \quad \underline{k}_T = \alpha k_T$$

$$\underline{\tilde{R}} = \tilde{R}/\rho_0 u, \quad \underline{\tilde{R}}(\underline{s}) = \frac{\underline{s}}{\underline{k}_L} + 4\beta^2 \frac{\underline{k}_T^2 - \underline{k}_T \underline{k}_L}{\underline{s} \underline{k}_L}$$

For simplicity we shall drop the underlining since from now on we shall only deal with the normalized variables.

To study the stability of equ. 1 we shall use the method of the determinant presented in ref. 4. The function D(s) is defined as

$$D(s) = 1 - \sum_{\ell=0}^{\infty} (-1)^{\ell} \sum_{k=-\infty}^{+\infty} G(s+ik\Omega)G(s+ik\Omega+2i\Omega)\dots G(s+ik\Omega+2i\ell\Omega)$$

where  $G(s) = g(s) g(s + i\Omega)$  (3)

$$g(s) = \frac{\beta/2}{\beta + \gamma s \tilde{R}(s)}$$

There is stability if D(s) has no zeroes in the half plane  $\text{Re } s > 0$ . When there are zeroes in  $\text{Re } s > 0$  the real part of the zeroes gives the growthrate of the instability.

Nyquist diagrams

$D(s)$  has the following properties

$$D(s^*) = D^*(s) \quad , \quad D(s + i\Omega) = D(s) \quad , \quad D(+\infty) = 1 \quad (4)$$

It is analytic in  $\text{Re } s > 0$ . From these relations it follows that  $\text{Im } D(x + in\Omega) = 0$ .

The curve obtained by joining the points  $D(iy)$  for  $0 \leq y \leq \Omega/2$  can be called a Nyquist diagram although the curve is not the image of a closed contour in the  $s$  plane. The number of times the curve, closed by its complex conjugate, encircles the origin, gives the number of zeroes in any band  $\text{Re } s > 0, y_0 \leq \text{Im } s \leq y_0 + \Omega$  ( $y_0$  arbitrary). Ref. 5 gives more details on the use of such diagrams in more complicated cases.

In this simple case there are only four types of Nyquist diagrams:

- stable:  $D(0) > 0, D(i\Omega/2) > 0$  and the curve does not encircle the origin. This is the only stable case.
- M-unstable:  $D(0) > 0, D(i\Omega/2) > 0$  and the curve encircles the origin once.  $D(s)$  has zeroes at  $s = x \pm iy + in\Omega$ .
- $\Omega$ -unstable:  $D(0) > 0, D(i\frac{\Omega}{2}) < 0$ .  $D(s)$  has zeroes at  $s = x + i\frac{\Omega}{2} + in\Omega$ .
- 0-unstable:  $D(0) < 0, D(i\frac{\Omega}{2}) > 0$ .  $D(s)$  has zeroes at  $s = x + in\Omega$ .

In these equations  $n$  is an integer,  $x$  and  $y$  are positive;  $x$  is the growthrate of the instability.

Results

There are only two parameters in the problem:  $\beta$  and  $\Omega$ . Fig. 1 shows in the plane  $\beta$ - $\Omega$  the regions of instability for  $\gamma = 1$ .

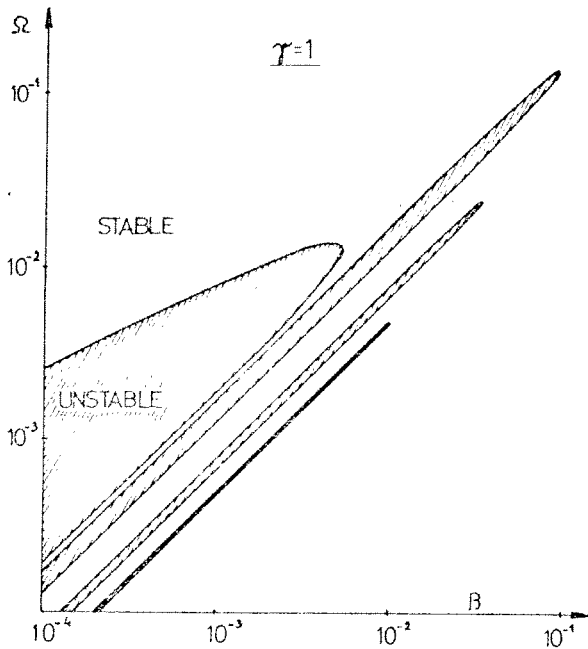
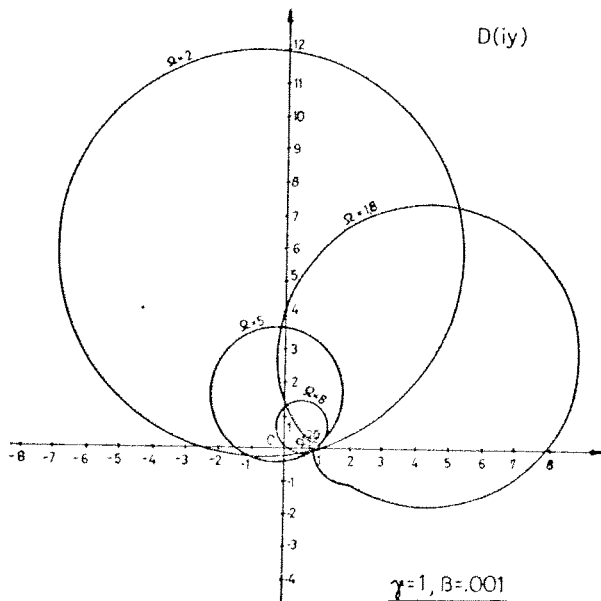


Fig. 1 Stability diagram for  $\gamma = 1$ . The regions hatched are unstable. Only the first three parametric instability regions are shown:  $n = 1, 2, 3$ .

There is an infinite number of these needle shaped unstable regions all parallel to the first three shown. They are very narrow and centered around  $\Omega \approx \frac{1.45}{n} \beta$ . As  $n$  increases these needles recede to the left, continuing the trend already visible on the first three. Above these needle shaped regions there is a wide unstable region which grows as  $\beta$  decreases, in contrast to the "needles" which assume a constant width at small values of  $\beta$ .



To gain some understanding of these diagrams let us look at the Nyquist diagrams in the various regions. Fig. 2 shows how

Fig. 2 Nyquist diagrams for  $\gamma = 1, \beta = .001$ . The values of  $\Omega$  written on the diagram have to be multiplied by  $10^{-3}$ .



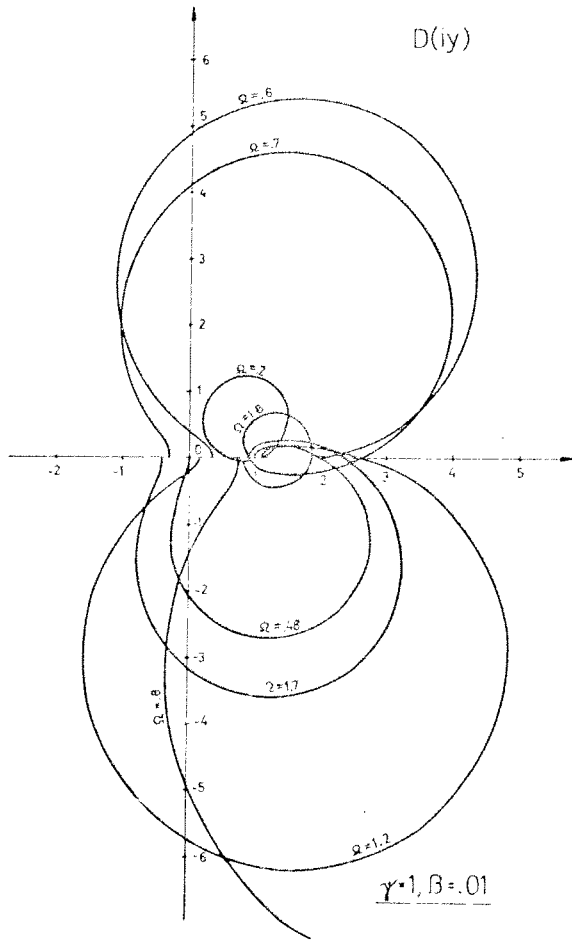


Fig. 3 Nyquist diagrams for  $\gamma = 1, \beta = .01$ . The values of  $\Omega$  have to be multiplied by  $10^{-2}$ .

the first unstable region develops as  $\Omega$  decreases, for a fixed value of  $\beta$ . It shows that the first region is M-unstable. Fig. 3 shows that in the first two needle shaped regions the diagrams are  $\Omega$ - or O-unstable respectively. If one identifies each region by the value of  $n$ , the odd regions are  $\Omega$ - unstable and the even ones O-unstable.

The stability diagram for  $\gamma = 5/3$  is shown in Fig. 4. It shows very few differences from the stability diagram with  $\gamma = 1$ . There is a reduction in the extent of the large instability region and a slight change in the location of the needle shaped regions, which are now given approximately by  $\Omega \approx 1.2\beta/n$ . The end points of these needle shaped regions for  $\gamma = 1$  and  $\gamma = 5/3$  correspond almost to the same frequency.

From the two stability diagrams we can conclude that stability of all modes is achieved for  $\Omega > .13$ , which corresponds to a true frequency  $f = \frac{2\pi}{\omega} \approx .01v$ . Using the results of Braginskii (6) to relate  $v$  to  $v_i$ , the ion collision frequency, it gives  $f \approx .02v_i$ .

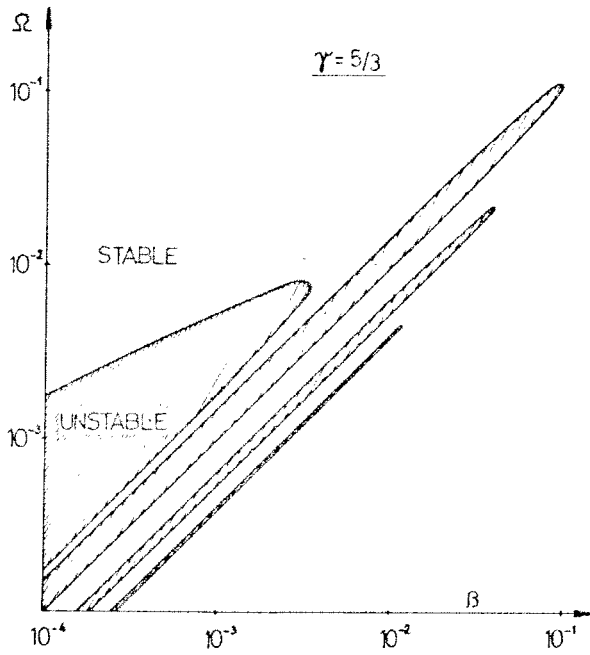


Fig. 4 Stability diagram for  $\gamma = 5/3$ . The hatched regions are unstable. Only the first three parametric regions are shown:  $n = 1, 2, 3$ .

Interpretation of the results

Consider the hypothetical system described by equ. 1 without the  $\cos 2\omega t$  term. We shall call this system the average system ( $\cos 2\omega t$  term averages to zero). The dispersion relation for this system is simple for  $\beta \ll 1$ :

$$\beta + \frac{\gamma s^2}{\sqrt{\beta^2 + s^2}} = 0 \tag{5}$$

which has the solutions  $s_0 = \pm i\beta \sqrt{\frac{2}{1 + \sqrt{1 + 4\gamma^2}}}$ . The average system has an undamped resonance at the frequency  $|s_0|$ . For  $\gamma = 1$ ,  $|s_0| \approx .79 \beta$  and for  $\gamma = 5/3$ ,  $|s_0| \approx .67 \beta$ . We expect the oscillating term to pump energy into this mode and drive

it unstable whenever  $\Omega \approx \frac{2|s_0|}{n}$  ( $n = 1, 2, \dots$ ). We have indeed found unstable regions whenever  $\Omega \approx \frac{1.8|s_0|}{n}$ . The difference in the coefficient is not important and reflects the fact that equ. 1 is not a Mathieu equation. We can conclude that the needle shaped regions are parametric excitations of a weakly damped mode of the average system.

The existence of the region of instability for  $\Omega \gg 2|s_0|$  and  $\beta \ll 1$  was already uncovered in ref. 4. Since in the case of a Mathieu-Hill equation there is always stability for  $\Omega \gg 2|s_0|$  (where  $s_0$  is the resonance frequency of the system without the oscillating term), it is of interest to try to understand this difference in behavior.

The determinant  $D(s)$  (equ. 3) can be written as

$$D(s) = 1 - g(s) D_1(s) - D_2(s) \quad (6)$$

where  $D_1(s)$  and  $D_2(s)$  depend only on  $g(s+ik\Omega)$ ,  $k \neq 0$ .

We generalize the definition of  $g(s)$ <sup>4</sup>:

$$g(s) = \frac{A/2}{X + s\tilde{Z}(s)}$$

$\tilde{Z}(s)$  can be any response function which satisfies the three conditions:

$\tilde{Z}(s)$  holomorphic in  $\text{Re } s > 0$ ,  $\text{Re } \tilde{Z}(s) > 0$  for  $\text{Re } s > 0$  and  $\lim_{|s| \rightarrow \infty} \tilde{Z}(s) > 1$ .

$|s| \rightarrow \infty$

The roots of  $D(s)$  satisfy the equation

$$X^* + s\tilde{Z}^*(s) = 0$$

$$X^* = X - \frac{A}{2} \frac{D_1(0)}{1 - D_2(0)}, \quad X^* \text{ real} \quad (7)$$

$$\tilde{Z}^*(s) = \tilde{Z}(s) - \frac{A}{2} \frac{D_1(s) - D_1(0)}{s(1 - D_2(s))} - \frac{A}{2} \frac{D_1(0)\{D_2(s) - D_2(0)\}}{s(1 - D_2(0))(1 - D_2(s))}$$

The dispersion relation with the oscillating term is thus reduced to the dispersion relation without the oscillating term, with modified values of  $X$  and  $\tilde{Z}(s)$ . This is just a formal transformation of the equation  $D(s) = 0$ . For  $|\text{Im}s| \leq \Omega/2$  and  $\Omega$  sufficiently above all possible parametric excitation frequencies,  $|D_2(s)| \ll 1$ ,  $|D_1(s)| \ll 1$  and the equations for  $X^*$  and  $Z^*(s)$  simplify

$$X^* \approx X - \frac{A}{2} D_1(0)$$

$$Z^*(s) \approx Z(s) - \frac{A}{2} \frac{D_1(s) - D_1(0)}{s}$$

We have also assumed that  $|D_2'(s)| \ll 1$ .

For our case  $A = X = \beta$  and  $\tilde{Z}(s) = \gamma \tilde{R}(s)$ . We limit the range of  $\Omega$  to  $\beta \ll \Omega \ll 1$ . In this range  $\tilde{R}(j\Omega) \approx 1$  and  $X^*$ ,  $\tilde{Z}^*(s)$  reduce to

$$X^* \approx \beta$$

$$\tilde{Z}^*(s) \approx \tilde{R}(s) - \frac{\beta^2}{2\gamma\Omega^2}$$

The oscillation has the same effect as adding an active element to the static system (negative resistance). It is noteworthy that by choosing a frequency  $\Omega$  in the range where the plasma behaves as a completely passive element ( $\tilde{R}(j\Omega) = 1$ !) has the same effect as adding a negative resistance to the static system. By solving equ.(7) we find for the upper stability boundary

$$\Omega^2 = \frac{3\gamma\beta}{2(1 + 6\gamma^2) (1 + \sqrt{1 + 4\gamma^2})}$$

At this frequency the damping in  $\tilde{R}(s)$  just balances the negative resistance and the oscillation at the frequency  $|s_0|$  (equ. 5) is undamped. At a lower frequency the mode given by equ. (5) is driven unstable.

In the case where  $\tilde{R}(s) \sim s$  at large frequencies we find for large values of  $\Omega$

$$X^* \approx X + \frac{A^2}{2\Omega^2}$$

$$\tilde{Z}^*(s) \approx \tilde{R}(s)$$

The oscillating term has clearly a stabilizing influence.  $\tilde{R}(s)$  is unaffected at this order by  $A$ . These formulas give identical results to the conventional quasi-potential approximation<sup>7</sup>, in the restricted case where  $\tilde{R}(s) = s$  for all  $s$  (Mathieu equation). In conclusion we have shown that the stability diagram obtained numerically can be interpreted physically. The method presented to study the high frequency limit is very general and reduces to the usual quasi-potential approximation for the special case of a Mathieu equation.

Growthrates

Because of the high value of the frequency needed to achieve stability of all modes, it is of interest to find the growth-rates of the instabilities at lower frequencies. Just by looking at the diagrams it is clear that the  $n = 1$  parametric instability must be the fastest growing mode since it is the hardest to suppress,  $n = 2$  being the next highest. Fig. 5

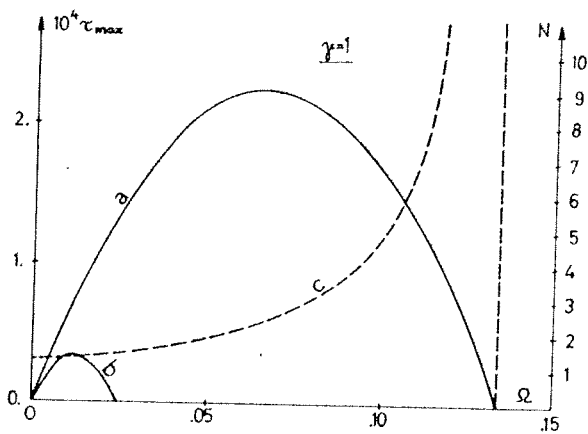


Fig. 5 Growthrates of the most unstable modes in the first two parametric instability regions for  $\gamma = 1$ . The curve a is for  $n = 1$  and b for  $n = 2$ . The dotted curve c is the growthtime of the mode a in number of periods of the applied field. The ordinate for the curves a, b is to the left.  $\tau_{max}$  is also normalized to  $u/\alpha$ . The right ordinate N refers to curve c.

shows the fastest growth-rate as a function of the applied frequency  $\Omega$  for  $\gamma = 1$  in the two regions  $n = 1$  and  $n = 2$ . The mode  $n = 1$  is by far the fastest growing. The dotted line shows  $N(\Omega) = 4\pi/(\Omega\tau_{max})$ , that is the growthtime of the worst instability expressed in number of periods of the applied field. This curve shows that the growthtime is of the order of a period. This is a strong instability. Unless there is a powerful non-linear mechanism to stop the growth of this instability, it appears hopeless to try to use a frequency appreciably below .01v .

The results for  $\gamma = 5/3$  are almost identical and introduce nothing new to the discussion.

Limits of validity of the calculation

The use of the model is justified<sup>4</sup> if  $\beta > \sqrt{\frac{\alpha}{a}}$ , where  $a$  is the plasma radius, and if  $\alpha \ll a$ . For all fluid models  $\beta$  and  $\Omega$  should be limited to  $\beta, \Omega \ll 1$ . We found stability only at a frequency  $\Omega \gtrsim .13$ . Although there is no doubt that the increase in damping as  $\beta$  approaches 1, which makes it possible to obtain stability, is real, can this value of  $\Omega$  be reliable? This condition can be rewritten as  $2f \gtrsim .04v_i$ . The wavelength of the last unstable mode is equal to  $\approx 65a$ . In this range of frequency and wavelength the fluid model should still be valid.

Acknowledgments

This work was performed under the auspices of the Swiss National Science Foundation.

References

1. I.R. JONES, A. LIETTI, J.-M. PEIRY Plasma Physics 10, 213  
(1968)
2. A. BERNEY, A. HEYM, F. HOEMANN, I.R. JONES  
(to be published)
3. E.S. WEIBEL Phys.Fluids 3, 946 (1960)
4. F. TROYON Phys.Fluids 10, 2660  
(1967)
5. F. TROYON (to be published) and LRP  
41/70
6. S.I. BRAGINSKII Soviet Physics JETP, 6  
(33), 358 (1958)
7. G.H. WOLF Zeitschrift für Physik,  
227, 291 (1969)